Drug Repurposing Effort for the Novel Acetylcholinesterase and Butyrylcholinesterase Targets: A Combined in Silico and in Vitro Study

Hind Aljanabi[1], Murat Şentürk[2], Barbaros Nalbantoğlu[1*]

[1] Department of Chemistry, Faculty of Arts and Sciences, Yıldız Technical University, Istanbul, Turkey

[2] Department of Basic Sciences of Pharmacy, Pharmacy Faculty, Agri Ibrahim Cecen University, Agri, Turkey,

h.aljanabee@yahoo.com

barbaros@yildiz.edu.tr

msenturk@agri.edu.tr

***Corresponding Author :** Prof. Dr. Barbaros NALBANTOĞLU (barbaros@yildiz.edu.tr)

Abstract: In the current drug repurposing study, 7822 small compounds were fetched from NIH small molecule library and are screened through a binary Alzheimer's Disease (AD)-QSAR model. The cut-off value for AD therapeutic activity set as (>0.75), and the molecules with higher values identified and then tested in the 26 different toxicity-QSAR models. Selected hits with no predicted toxicities were then interacted with acetylcholinesterase (AChE), and butyrylcholinesterase (BuChE) targets using combined molecular docking and molecular dynamics (MD) simulations. Our in silico screening results identified five hit compounds: Ocaperidone, cafedrine, isosulpride, risperidone, and nelfinavir. Three of these compounds together with FDA approved compounds against AD were used in in vitro tests against AChE and BChE, and our experimental results confirmed in silico predictions. All of three selected hits (ocaperidone, risperidone, and nelfinavir) represented nM-level IC50 values for both AChE and BChE targets. The results of the conducted drug repurposing study may open a new perspective for the development of novel small molecule cholinesterase inhibitors.

Key words: Alzheimer disease, cholinesterase inhibitors, molecular docking, butyrylcholinesterase, MD simulations, acetylcholinesterase, drug repurposing.
Tob Regul Sci.™ 2021;7(6-1): 7050-7064
DOI: doi.org/10.18001/TRS.7.6.1.34

1. Introduction

Alzheimer's disease (AD) is a type of irreversible brain disease that creates memory, consideration, and behavior problems. AD affects around 50 million people worldwide and gets worse with severe behavioral and psychological symptoms over the long term (Wu, et al. 2017). Symptoms first appear in most people with AD in their mid-60s (Kurt, et al. 2017). Scientists keep sorting out the complex brain changes involved with AD onset and progression. It seems that brain changes may start a decade or more before memory and other cognitive issues ocur (Kurt, et al. 2017). People appear to be free of symptoms during this preclinical stage of AD, even though some toxic changes are taking place in the brain.

Neurological changes associated with AD include sediments of abnormal, stable, and insoluble protein throughout the brain. These sediments will form what is called amyloid plaques, and tau tangles and healthy neurons will stop working, lose connections, and die with other neurons (Kurt, et al. 2017). It is also thought that many other complex brain changes will play a role in AD. So far, scientists could not predict what the actual causes (i.e., exact etiology) behind AD are, however, the disease exhibits some associations with a combination of factors related to genetics, environment, and lifestyle.

Although AD is is now listed as the sixth highest cause of mortality in the United States, recent projections imply that it may be the third largest cause of death for olders, trailing only heart disease and cancer. (Matthews, et al. 2019).

AD is generally characterized by a deficiency in the amount of neurotransmitter acetylcholine (ACh) in the brain. Therefore, inhibitors of cholinesterase (ChE) are the first-line pharmacological agents used to treat AD.2 Damage to the cholinergic neurotransmission that produces ACh has been shown to be related to memory disorders in patients with AD. Some of the cognitive habits were correlated with ACh existing in the brain cortex and plasticity (Lane, et al. 2006; Thompson, et al. 2012).

The enzyme class of ChE consists primarily of two target proteins, namely, acetylcholinesterase (AChE, E.C. 3.1.1.7) and butyrylcholinesterase (BChE, E.C. 3.1.1.8). The sequence identity between the AChE and BChE is very high (nearly 84%), so the responses they give each other are matching (Chen, et al. 2017). They are mostly present in the central nervous system and cholinergic synapses in vertebrates (Orhan, et al. 2018).

AChE regulates various physiological processes by hydrolyzing ACh and converting it to cholinergic synapses. BChE, on the other hand, is found in the stomach, liver, heart, kidney, lungs, and serum and is expressed in neuroglia. It is important in the metabolism of compounds containing ester.ACh may also be hydrolyzed, and its level does not decrease, or it can even rise in AD. AChE is usually prevalent in the brain, but BChE activity increases when AChE activity stays unchanged or decreases in AD patients. The cessation of cholinergic signaling by hydrolyzing ACh is responsible for both enzymes. Therefore, a medication that inhibits both AChE and BChE can be preferable. Indeed, it is shown that blocking both AChE and BChE together may reduce the formation Aβ plaques (Auld, et al. 2002).

The US Food and Drug Administration (FDA) has approved five drugs for the treatment of AD so far. Rivastigmine, tacrine, galantamine, and donepezil are AChE antagonists, while memantine is an antagonist of the N-methyl-D-aspartate (NMDA) receptor (Auld, et al. 2002). AChE inhibitors with a license prevent metabolite products from developing in ACh. AD is caused by low levels of the neurotransmitter ACh in the synaptic cleft. Nonetheless, current ChE inhibitors have several drawbacks, such as bradycardia, syncope, nausea, diarrhea, anorexia, migraine, sleeplessness, and muscle cramps, as well as other adverse effects. (Deardorff, et al. 2015; Mirjana, et al. 2013). The current therapies only prolong the development of AD-related symptoms. Hence, the need for effective treatment is crucial.

Recent development in computational biology approaches and molecular modeling techniques lead new opportunities for the detection, diagnosis, and design/development of more effective treatments against both common and rare diseases. Many data types, including molecular, medical, and epidemiological data, are becoming publicly available at comparable rates. It is possible to use these databases including small molecule libraries against specific target proteins to find new uses for existing therapies (Baker 2012; Huang, et al. 2011).

The aim of this study is to reveal the potential use of new small known molecules against AD which were previously used against for different biological problems. For this aim, a small molecule library (around 7900 compounds) which

has approved drugs (around 22% of the library) and compounds tested in clinical phase studies (around 78% of the library) is virtually screened initially in ligand-based AD model, then at the binding sites of BChE and AChE, which play an essential role in AD, and targeting these enzymes are one of the applied therapy. We not only wanted to find therapeutic compounds that target AChE and BChE, but we also wanted to know about the pharmacokinetic characteristics and toxicity of the hit ligands. Selected hits based on multiscale ligand and structure-driven approaches aid in the discovery of novel hits relevant to AChE and BChE targets. In vitro tests were used to test the selected hit compounds.

2. Materials and methods

Small molecules approved for use as medications can be "repurposed" to new uses to establish the causes of their beneficial and adverse effects. The assembly of identified and registered small molecule drugs (7822 FDA approved and compounds in clinical trials) has been retrieved from the NIH's Chemical Genomics Center (NCGC) NPC database (Huang, et al. 2011) (downloaded on July 2018 from https:/tripod.nih.gov/npc). NPC's extensive collection of all human-approved small-molecule drugs would be invaluable for systemic human disease repurposing, especially for rare and neglected diseases, for which the cost and time needed to develop a new chemical entity is often prohibitive (Huang, et al. 2011).

2.1. Screening of Database in AD-QSAR Model

The collected small molecule database was first scanned for their therapeutic activity potentials against Alzheimer's Disease binary QSAR (AD-QSAR) using MetaCoreTM/MetaDrugTM platform of Clarivate Analytics (https://portal.genego.com). AD-QSAR model was used for the prediction of the therapeutic activity values of screened ligands. Training set of the model includes all possible compounds such as compounds with in vivo activity , approved drugs, and drug candidates in clinical trials. The model performance was evaluated by Cooper statistics parameters: sensitivity, specificity, accuracy, and MCC. (https://portal.genego.com). The "Therapeutic Activity Prediction (TAP)" predicts the activity of screened ligands using AD-QSAR. The predicted activity values from QSAR model are normalized to values between 0 and 1. (i.e., higher than 0.5 indicates the potential therapeutic activity). In our analysis, the AD-QSAR model was used with a cut-off value of TAP of ≥ 0.75. Screening results showed that 1326 out of 7822 molecules were found to have a larger TAP value than 0.75 in the AD-QSAR model. These molecules were then subjected to 26 different toxicity-QSAR models including cardiotoxicity, neurotoxicity, hepatotoxicity in which we observed that only 10 molecules out of 1326 showed no toxicity prediction. Thus, these selected ligands were used in target-driven-based studies.

2.2. Ligand preparation

The ligand preparation and geometry optimizations of all chosen 10 hits as well as positive control molecules were conducted using LigPrep module of Maestro using OPLS2005 force field. Epik module (Shelley, et al. 2007) was used to generate ionization states at neutral pH.

2.3. Protein Preparation

The crystal structure of target proteins was fetched from protein data bank (PDB). Following structures were used as target protein: AChE (ID: 4EY7) (Cheung, et al. 2012) and BChE (ID: 5DYW) (Košak, et al. 2016). The bond orders of target proteins are assigned and the missing residues in the protein (e.g., missing atoms and hydrogen atoms) were added using the crosslink proteins tool. Water molecules play important role in hydrogen bonding network, thus nearby water molecules (e.g., 5.0 Å of the ligands) were kept, and others were removed. The pKa prediction and protonation states of residues at the target proteins were conducted at physiological pH (7.4). PROPKA (Li, et al. 2005; Madhavi Sastry, et al. 2013) was to identify the protonation states of residues. Finally, restrained minimization (with 0.30 Å RMSD heavy atom convergence) was conducted with an OPLS2005 force field.

2.4. Grid Generation

Prepared protein structures were used in grid generation for molecular docking. Grid centers were -14.07, -43.93, and 27.92 and -5.33, 10.63, and -12.73 for x, y, and z coordinates, for AChE (4EY7) and BChE (5DYW) respectively. Glide sets inner box to 10x10x10 and outer box respect to the ligand size. The outer box dimensions were 27.82x27.82x27.82 and 25.18x25.18x25.18 for AChE (4EY7) and BChE (5DYW) respectively.

2.5. Molecular Docking Simulations of Selected Hits

Three different molecular docking algorithms (Quantum Mechanics-Polarized Ligand Docking (QPLD), Glide/ Standard Precision (SP), and Glide/ Induced Fit Docking (IFD)) were used for selected hit molecules from MetaCore/MetaDrug for docking calculations (Friesner, et al. 2004; Sherman, et al. 2006). Initially, Glide/SP docking program was used in to predict binding poses of the ligands at the binding site and calculate binding energies for the studied ligands towards AChE and BChE targets. The docking procedure predicts the low energy conformational matching of ligands (bioactive conformers) and their predicted binding free energies at the active site of targets (Cho, et al. 2005; Ekhteiari Salmas, et al. 2017; Gschwend, et al. 1996). Using the Glide docking program which is a grid-based approach, all ligands were docked into the AChE and BChE binding pockets, and 20 docking poses were requested for each ligand.

IFD approach assists in increasing the conformational sampling for both the residues at the binding pocket and ligand structures (Sherman, et al. 2006). Standard virtual docking experiments expect a rigid receptor, but in fact, several receptors adjust their binding position to adapt to the ligand's binding mode. This methodology is named as induced-fit docking, which is one of the most significant complicating factors in product design dependent on structure. It manages following protocols: i) all the inhibitors were docked into binding site of the AChE and BChE using Glide/SP, and high scored protein-ligand complexes were selected. ii) The docking poses within 5 Å from the docked conformations were refined (i.e., energy minimization was conducted) using Prime. iii) Finally, all the ligands were re-docked into the energy-minimized, refined binding domain of the targets using Glide/XP docking protocol. All ligands were docked into the AChE and BChE binding pockets with IFD approach, and 20 docking poses were constructed for each ligand.

QPLD was also used in the docking (Cho, et al. 2005). In this approach, before the single point energy calculation, partial atomic charges of each ligand are treated with ab initio methods. In this way, the receptor accounts for the polarization of the charges on the ligand, and the redocking of the ligands with these new partial charges may contribute to better docking precision (Cho, et al. 2005). The procedure operates by taking with highest-scoring poses of each ligand, measuring charges using QSite, redocking each of these poses, and choosing the best poses from the list. For the QM calculations, B3LYP density functional and 6-31G*/LACVP* basis set was used. In MD simulations, IFD poses were used as starting structures.

2.6. Molecular Dynamics (MD) simulations and Molecular Mechanics Generalized Born Surface Area (MM/GBSA) free energy calculations

Short (50 ns) and long (100 ns) MD simulations were conducted using the Desmond (Bowers, et al. 2006) to examine the structural and dynamical properties of ligands at the binding pocket of target proteins for top-IFD poses (in total, 1800 ns MD simulations were performed). Top-IFD poses of selected hits were solvated in an orthorhombic simulation box and systems were neutralized with required amount of Na+ and Cl- ions. Moreover, neutralization of the simulation system was achieved by adding 0.15 M NaCl to the simulation box. SPC solvent model was used in MD simulations. Before starting the production MD simulations, relaxation protocol for equilibration of the complexes was performed. The initial temperature was set as 310 K during simulations and regulated using the Nose-Hoover thermostat (Hoover 1985; Nosé 1984). The pressure was set to 1.01325 bar, and it is restricted by the

Martyna-Tobias-Klein system (Martyna, et al. 1994). An isothermal–isobaric (NPT) ensemble was used in MD simulations. OPLS2005 forcefield was used in MD simulations. Other settings were used as default. The MM/GBSA approach implemented in the Prime was used to calculate the binding free energies for selected ligands (Abel, et al. 2017; Hou, et al. 2011). Derived trajectory frames throughout the MD simulations (i.e., 100 frames for each simulations) were used in MM/GBSA. More clearly, 100 and 200 frames were extracted from the 50 ns and 100 ns MD simulations trajectories, respectively. The MM/GBSA system finds extensive use in the measurement of free energy of ligands at the binding pockets, and MM/GBSA produces better performance than docking (Hou, et al. 2011).

2.7. Average Structures

Obtained trajectories were opened in VMD. RMSD trajectory tool was used to align system respect to their backbone atoms. Then, RMSD graph of the system were plotted respect to the average structure. The closest frame to the average structure selected and exported (the frame that has the lowest RMSD respect to the average structure) , and used in representative structure figures.

2.8. In vitro activity tests for cholinesterase enzymes

Since we found that 5 out of 10 selected hit compounds show promising binding free energy results at both AChE and BChE targets, in vitro tests were considered for these compounds. Two of the compounds selected for in vitro experiments (cafedrine and isosulpride) could not be purchased due to the high prices of the active ingredients. Thus, we ordered three identified hits by our in silico drug repurposing study (i.e., ocaperidone, risperidone, and nelfinavir) from the available small molecule library. Selected 3 hit compounds were used in in vitro tests against AChE and BChE targets. The inhibitory activities were calculated according to Ellman's method (Ellman, et al. 1961). For this study, donepezil, an AChE inhibitor, was used as a reference molecule. IC50 values obtained for selected molecules with constructing absorbance and inhibition % curves. Stock solutions of molecules used in this study were prepared by dissolving them in dimethyl sulfoxide to be 1 mg/ml. It was then diluted to different concentrations using pure water. Six serial dilutions of these substances were measured to determine the inhibition activity of cholinesterase enzymes. The method used in this study has been explained in detail in previous studies (Cavdar, et al. 2019; Sahin, et al. 2020; Zilbeyaz, et al. 2018).

3. Results and Discussion

Although the pathophysiology of Alzheimer's disease is yet unknown, the reduced rates of acetylcholine (ACh) and butyrylcholine (BCh) found in the brains of AD patients are one of the most significant hypotheses. Inhibition of the enzymes AChE and BChE, which hydrolyze the neurotransmitters ACh and BCh, can thus be considered a therapeutic strategy. Hence, the inhibitory function for certain enzymes implicated in AD pathogenesis has been studied by several research groups (Ekins, et al. 2005; Ekins, et al. 2006; Myshkin, et al. 2012).

In recent years, repurposing/repositioning of medications has been increasingly common, as the designing the new compounds and transferring them to the clinical trials from scratch is financially costly and needs several years. In this work, we screened compounds at the binding pockets of AChE and BChE that are already approved by FDA as well as compounds under clinical trials. The NPC small molecule library from NIH, which has 7822 molecules was used for this aim.13 Among them 1751 compounds were FDA approved and 6171 were small compounds which were tested in clinical phase studies. Together with identification of new hit compounds from the FDA approved small molecule library, our goal was also to find and analyze small hit ligands with new scaffolds for AChE and BChE inhibition. Scheme 1 summarizes all of the procedures used in the current study for virtual screening workflow.

3.1. Therapeutic Activity, Docking and Pharmacokinetic Profiles of Screened Compounds

MetaCoreTM/MetaDrugTM (https://portal.genego.com) is an integrated software package that is used to predict the pharmacokinetic and toxicity properties of the molecules under investigation using a comprehensive system biology analysis package with the help of existing ADME, toxicity and disease -QSAR models. We initially used binary Alzheimer's Disease QSAR (AD-QSAR) model (Ekins, et al. 2005; Ekins, et al. 2006; Myshkin, et al. 2012). The AD-QSAR model predicts the therapeutic activity of screened compounds. The model normalizes the activity prediction between 0 and 1 (i.e., the value of >0.5 may be interpreted as potential therapeutic activity). Here, in order to focus only to promising potent compounds, we used a higher cutoff value (0.75) of predicted therapeutic activity score. We screened 7822 compounds at the AD-QSAR model and 1326 compounds showed the predicted therapeutic activity values of equal or higher than 0.75.

Although we used FDA approved compounds and compounds in clinical trials, together with therapeutic activity values, ADME/Toxicity predictions were also investigated since percentage of compounds in clinical trials among the library were high (78%). Thus, we used 26 different toxicity QSAR models in MetaCoreTM/MetaDrugTM and results showed that out of 1326 compounds, only 10 of them have high AD therapeutic activity and no predicted toxicity in all of the 26 toxicity QSAR models. Within 10 compounds, 2 of them (Nelfinavir and Risperidone) were FDA approved compounds and other 8 compounds were the small molecules used in clinical trials. Table 1 shows docking scores of selected hit compounds and three positive control molecules (i.e., donepezil, neostigmine and rivastigmine) at the active sites of AChE and BChE. Since the selected compounds and reference molecules have different sizes (i.e., molecular weights are different), we also calculated ligand efficiency scores (i.e., docking scores per nonhydrogen atoms) for each compound. (Table 1)

Figure 1 depicts the top-docking poses of nelfinavir which the one of the selected hit compounds at the AChE and BChE binding sites. Results show that nelfinavir forms π-π stacking interactions with Trp286, hydrogen bonds with Tyr72, Asp74, Ser293 and Arg296 via water bridges and hydrophobic interactions with following residues Tyr72, Leu76, Tyr77, Pro78, Tyr124, Trp286, Leu289, Val294, Phe297, Phe338, Val340, and Tyr341. It forms hydrogen bonds with Ser287, Asn289, Tyr332, and water-bridge interactions with Ser198 at the binding pocket of BChE. Hydrophobic contacts of nelfinavir are formed with Phe73, Trp82, Ala199, Trp231, Pro285, Leu286, Val288, Ala328, Phe329, Val331, Tyr332, Phe398, and Trp430. (Figure 1)

Toxicity profiles of selected top-5 docking scored compounds (based on AChE induced fit docking (IFD) scores), was represented at Table S1. Although selected hit compounds show no predicted toxicities, reference compounds represented high toxicities in some of the toxicity-QSAR models. For example, the donepezil showed high predicted toxicity risks for the following models: Cardiotoxicity, liver necrosis, liver cholestasis, liver weight gain, and genotoxicity). Indeed, clinical phase studies showed significantly higher incidence of bradycardia in patients receiving donepezil than controls (Howes 2014; Ogura, et al. 2000). Moreover, clinical study results showed that QT prolongation and torsades de pointes ventricular tachycardia during donepezil therapy is observed in two cases and the QT segments in both cases returned to normal when the donepezil was ceased (Howes 2014).

Table S2 compares predicted pharmacokinetic profiles of selected hit compounds including blood-brain barrier (BBB), human serum protein binding percentage, affinity to human serum albumin, and hERG blockage. Results showed together with donepezil, ocaperidone, risperidone, and isosulpride may permeate BBB. The selected hit compounds show high lipophilicity and they do not block the hERG channel. They also show moderate human serum protein binding profiles, while nelfinavir and cafedrine showed lower binding profiles. The calculated pharmacokinetic properties of selected hits show no crucial side effects.

3.2. Molecular Dynamics (MD) simulations

Ten hit compounds identified by ligand-based approaches were used in target-driven based analyses. These ligands were prepared and docked them to AChE and BChE targets using different docking approaches as explained in Methods chapter. (Table 1) Not only the docking scores but also the ligand-crucial residue interactions were investigated for the selected hits. Based on these analyses, we decided to carry out following five selected hits for further analyses: Ocaperidone, cafedrine, isosulpride, risperidone, and nelfinavir. In order to remove the risks for the affinity-biased selection towards larger compounds, we also calculated ligand efficiency (LIE) scores (i.e., docking score/number of nonhydrogen atoms). We calculated LIE scores using Glide/IFD scores to achieve this goal. The isosulpride compound had the highest LIE values in both AChE and BChE, according to the results (-0.747 and -0.487 kcal/mol, respectively).

These selected 5 hits were then used in MD simulations. For this aim, top-docking poses from IFD were used as input complexes in MD simulations. Two different time scales were considered in MD simulations (50 ns and 100 ns) for the selected 5 hits as well as positive control compounds. The root mean squared deviation (RMSD)-time plots of the simulations for the protein has been shown at the Figures S1-S4. Results show that in both simulations (50 ns and 100 ns) for AChE and BChE complexes, simulation systems are equilibrated and RMSD values were not observed as more than 2.5 Å during the simulations. Two different RMSD plots (i.e., LigFitLig and LigFitProt) were considered for the ligands. While LigFitLig RMSD plots show the RMSD of a ligand that is aligned and measured to its reference conformation, LigFitProt RMSD plots show the RMSD of a ligand when the protein-ligand complex is first aligned on the protein backbone of the reference and then the RMSD of the non-hydrogen atoms of the ligand is measured. The LigFitProt RMSD results of the ligands at the AChE and BChE plots show that while nelfinavir has higher conformational changes compared to its reference binding mode at the AChE in both of 50 ns and 100 ns simulations, corresponding ligand was neostigmine at BChE. (Figures S5-S8) Figures S9 and S10 shows representative ligand mode of nelfinavir at the binding pocket of BChE and AChE. LigFitLig RMSD plots of the ligands represent that there are no any large internal structural changes (i.e., rotational) at the ligands throughout the simulations. (Figures S11-S14)

3.3. Water-bridge Interactions

Cafedrine, isosulpride, risperidone, and neostigmine molecules interacted with AChE through water network both in 50 and 100 ns simulations. Risperidone, nelfinavir, rivastigmine, and donepezil formed water bridge interactions with the BChE, during both 50 and 100 ns MD simulations. Risperidone was the only compound that formed and conserved water bridge interactions both with AChE and BChE during 50 and 100 ns MD simulations. (See Figures S17-S24).

Average binding free energy calculations were conducted by Molecular Mechanics Generalized Born Surface Area (MM/GBSA) method. Average MM/GBSA energies throughout the MD simulations were calculated for each ligand (Table S3). Average MM/GBSA scores show that identified 5 hit compounds have similar or even better predicted binding affinity profiles to the AChE and BChE targets compared to FDA approved small molecule drugs. 2D and 3D ligand interaction diagrams show that identified hit compounds constructs similar nonbonding chemical interactions with positive control inhibitors. Figure 2 shows a schematic of detailed ligand atom interactions with target protein residues for risperidone and donepezil at AChE and BChE targets. Interactions that presented more than 30% of the simulation time during the simulations are provided. While Asp74, Trp86, Trp286, Phe295, Arg296, Tyr337, and Tyr341 are found crucial residues for risperidone at the AChE, corresponding residues were Trp86, Trp286, Phe295, Tyr337, and Tyr341 for donepezil. Important contact residues were found as Trp82, Tyr332, Phe329, and His438 for risperidone at the BChE. Corresponding residues were Trp82, Gly115, Tyr128, Ala328, and Phe329 for donepezil. These results confirm that identified compounds and reference positive control molecules share similar residue/ligand contact maps.

3.4. In vitro cholinesterase activity of selected hits

To test and validate molecular modeling predictions and in silico studies based on hybrid ligand-dependent and target-driven approaches used in the current drug repurposing effort, three-hit molecules were ordered from AmBeed.com and similar protocol that we have conducted previously were performed (Cavdar, et al. 2019; Sahin, et al. 2020; Zilbeyaz, et al. 2018). The half maximal inhibitory concentration (IC50) values of three identified compounds (ocaperidone, risperidone, and nelfinavir) for the AChE and BChE targets were determined from different inhibitor concentrations (Table 2). Both AChE and BChE inhibitions are indicated by comparing the IC50 values of the three chosen molecules. To block both enzymes together, which are known to be crucial for AD, selected molecules can display a synergistic effect. The IC50 values of selected hits were in the range of 70.23 to 89.22 nM for AChE and 36.06 to 49.37 nM for BChE. (Figure S15).

Recently Almaz et al synthesized a sets of benzohydrazides derivatives and tested them experimentally. Moreover, they also performed molecular docking calculations to predict the binding affinities of their compounds at the binding pocket of AChE and BChE (Almaz, et al. 2021). The most potent compound, namely 3a was found to inhibit AChE and BChE, with 590 and 150 nanomolar affinities. Fais et al synthesized a sets of hydroxylated 2-phenylbenzofuran derivatives and biological binding tests were performed. The most potent compound against AChE and BChE was found as Compound 6 which has 23.96 μM and 7.96 μM affinities, respectively (Fais, et al. 2019).

Shaikh and colleagues synthesized alpha-aminophosphonate derivatives to inhibit AChE and BChE. The most potent compound was found as 4j, which has 0.475 μM and 3.306 μM, for the AChE and BChE, respectively (Shaikh, et al. 2020).

Selected hit molecules showed their inhibition effect in both enzymes, and their binding affinities are considered similar with the recognized drugs neostigmine and rivastigmine but less than donepezil. The best inhibition against AChE and BChE was found with nelfinavir (IC50 = 70.23 nM and 36.06 nM), respectively. These compounds can thus be used as lead compounds, and with molecular tailoring experiments, their binding affinities can be strengthened. Within the selected hits, ocaperidone and risperidone are antipsychotics primarily bind and with high affinity to 5-HT2 (serotonin) receptors, alpha1 and alpha 2 adrenergic receptors, dopamine D2 receptors and histamine H1 receptors. Risperidone is licensed for the short-term treatment of aggression in AD. Nelfinavir is a well-known human immunodeficiency virus (HIV-1) protease inhibitor. To the best of our knowledge, there is no previous clinical report showing nelfinavir's usage against AD.

3.5. Limitations of the Study

Liston et al showed that high selectivity for AChE over BChE, may help to achieve a clinically acceptable tolerability profile for Alzheimer's disease (Liston, et al. 2004). In our study, proposed compounds, ocaperidone, risperidone, and nelfinavir were not selective for AChE over BChE. However, since the proposed compounds have nanomolar activity for AChE and BChE, we expect lesser adverse effects due to cholinergic hyperactivity in line with the Weinstock's findings (Weinstock 1999) (More side effects are observed in the presence of only BChE inhibiting molecules).The same data or information given in a Table must not be repeated in a Figure and vice versa. It is not acceptable to repeat extensively the numbers from Tables in the text or to give lengthy explanations of Tables or Figures.

4. Conclusions

In this study, we used NPC approved and investigational drug library to repurpose existing drugs with less toxicity than the already used drugs in AD treatment. 7822 compounds first filtered using MetaCoreTM/MetaDrugTM server according to Alzheimer-QSAR model. Then, 1326 compounds were obtained as possible ligands. These molecules were tested in 26 different toxicity-QSAR models to eliminate the compounds with high toxicity, and finally, 10

compounds were retained. Moreover, conducted hybrid in silico approaches including docking, and MD simulations methods show that selected hits are structurally stable at the binding pockets of both targets. Both molecular docking and MD simulations were also conducted for known AChE and BChE inhibitors, and results showed that similar crucial residues at the binding pocket interacts with studied molecules and known inhibitors. Since we found that 5 out of 10 selected hit compounds show promising binding free energy results at both AChE and BChE targets, in vitro tests were considered for these compounds. Although all the identified compounds show nanomolar-range IC50 values in both target proteins, among them nelfinavir showed the most potent inhibition against AChE and BChE with IC50 values of 70.23 and 36.06 nM, respectively.

References

[1]. Abel R, Wang L, Harder ED, Berne BJ, Friesner RA (2017). Advancing Drug Discovery through Enhanced Free Energy Calculations. Accounts of Chemical Research 50:1625-1632 https://doi.org/10.1021/acs.accounts.7b00083

[2]. Almaz Z, Oztekin A, Tan A, Ozdemir H (2021). Biological evaluation and molecular docking studies of 4-aminobenzohydrazide derivatives as cholinesterase inhibitors. Journal of Molecular Structure 1244:130918 https://doi.org/10.1016/j.molstruc.2021.130918

[3]. Auld DS, Kornecook TJ, Bastianetto S, Quirion R (2002). Alzheimer's disease and the basal forebrain cholinergic system: relations to β-amyloid peptides, cognition, and treatment strategies. Progress in Neurobiology 68:209-245 https://doi.org/10.1016/S0301-0082(02)00079-5

[4]. Baker M (2012). Gene data to hit milestone. Nature 487:282-283 https://doi.org/10.1038/487282a

[5]. Bowers KJ, Chow DE, Xu H, Dror RO, Eastwood MP, Gregersen BA, Klepeis JL,

[6]. Kolossvary I, Moraes MA, Sacerdoti FD, Salmon JK, Shan Y, Shaw DE (2006) Scalable Algorithms for Molecular Dynamics Simulations on Commodity Clusters. In: SC '06: Proceedings of the 2006 ACM/IEEE Conference on Supercomputing, pp 43-43 https://doi.org/10.1109/SC.2006.54

[7]. Cavdar H, Senturk M, Guney M, Durdagi S, Kayik G, Supuran CT, Ekinci D (2019). Inhibition of acetylcholinesterase and butyrylcholinesterase with uracil derivatives: kinetic and computational studies. Journal of Enzyme Inhibition and Medicinal Chemistry 34:429-437 https://doi.org/10.1080/14756366.2018.1543288

[8]. Chen Z, Digiacomo M, Tu Y, Gu Q, Wang S, Yang X, Chu J, Chen Q, Han Y, Chen J, Nesi G, Sestito S, Macchia M, Rapposelli S, Pi R (2017). Discovery of novel rivastigmine-hydroxycinnamic acid hybrids as multi-targeted agents for Alzheimer's disease. European Journal of Medicinal Chemistry 125:784-792 https://doi.org/10.1016/j.ejmech.2016.09.052

[9]. Cheung J, Rudolph MJ, Burshteyn F, Cassidy MS, Gary EN, Love J, Franklin MC, Height JJ (2012). Structures of Human Acetylcholinesterase in Complex with Pharmacologically Important Ligands. Journal of Medicinal Chemistry 55:10282-10286

[10]. Cho AE, Guallar V, Berne BJ, Friesner R (2005). Importance of accurate charges in molecular docking: Quantum mechanical/molecular mechanical (QM/MM) approach. Journal of Computational Chemistry 26:915-931 https://doi.org/10.1002/jcc.20222

[11]. Deardorff WJ, Feen E, Grossberg GT (2015). The Use of Cholinesterase Inhibitors Across All Stages of Alzheimer's Disease. Drugs & Aging 32:537-547 https://doi.org/10.1007/s40266-015-0273-x

[12]. Ekhteiari Salmas R, Unlu A, Bektaş M, Yurtsever M, Mestanoglu M, Durdagi S (2017). Virtual screening of small molecules databases for discovery of novel PARP-1 inhibitors: combination of in silico and in vitro studies. Journal of Biomolecular Structure and Dynamics 35:1899-1915 https://doi.org/10.1080/07391102.2016.1199328

[13]. Ekins S, Andreyev S, Ryabov A, Kirillov E, Rakhmatulin EA, Bugrim A, Nikolskaya T (2005). Computational prediction of human drug metabolism. Expert Opinion on Drug Metabolism & Toxicology 1:303-324 https://doi.org/10.1517/17425255.1.2.303

[14]. Ekins S, Bugrim A, Brovold L, Kirillov E, Nikolsky Y, Rakhmatulin E, Sorokina S, Ryabov A, Serebryiskaya T, Melnikov A, Metz J, Nikolskaya T (2006). Algorithms for network analysis in systems-ADME/Tox using the MetaCore and MetaDrug platforms. Xenobiotica 36:877-901 https://doi.org/10.1080/00498250600861660

[15]. Ellman GL, Courtney KD, Andres V, Featherstone RM (1961). A new and rapid colorimetric determination of acetylcholinesterase activity. Biochemical Pharmacology 7:88-95 https://doi.org/10.1016/0006-2952(61)90145-9

[16]. Fais A, Kumar A, Medda R, Pintus F, Delogu F, Matos MJ, Era B, Delogu GL (2019). Synthesis, molecular docking and cholinesterase inhibitory activity of hydroxylated 2-phenylbenzofuran derivatives. Bioorganic Chemistry 84:302-308 https://doi.org/10.1016/j.bioorg.2018.11.043

[17]. Friesner RA, Banks JL, Murphy RB, Halgren TA, Klicic JJ, Mainz DT, Repasky MP, Knoll EH, Shelley M, Perry JK, Shaw DE, Francis P, Shenkin PS (2004). Glide: A New Approach for Rapid, Accurate Docking and Scoring. 1. Method and Assessment of Docking Accuracy. Journal of Medicinal Chemistry 47:1739-1749 https://doi.org/10.1021/jm0306430

[18]. Gschwend DA, Good AC, Kuntz ID (1996). Molecular docking towards drug discovery. Journal of Molecular Recognition 9:175-186 https://doi.org/10.1002/(SICI)1099-1352(199603)9:2<175::AID-JMR260>3.0.CO;2-D

[19]. Hoover WG (1985). Canonical dynamics: Equilibrium phase-space distributions. Physical Review A 31:1695-1697 https://doi.org/10.1103/PhysRevA.31.1695

[20]. Hou T, Wang J, Li Y, Wang W (2011). Assessing the Performance of the MM/PBSA and

[21]. MM/GBSA Methods. 1. The Accuracy of Binding Free Energy Calculations Based on Molecular Dynamics Simulations. Journal of Chemical Information and Modeling 51:69-82 https://doi.org/10.1021/ci100275a

[22]. Howes LG (2014). Cardiovascular Effects of Drugs Used to Treat Alzheimer's Disease. Drug Safety 37:391-395 https://doi.org/10.1007/s40264-014-0161-z

[23]. Huang R, Southall N, Wang Y, Yasgar A, Shinn P, Jadhav A, Nguyen D-T, Austin CP (2011). The NCGC Pharmaceutical Collection: A Comprehensive Resource of Clinically Approved Drugs Enabling Repurposing and Chemical Genomics. Science Translational Medicine 3:80ps16-80ps16 https://doi.org/10.1126/scitranslmed.3001862

[24]. Košak U, Brus B, Knez D, Šink R, Žakelj S, Trontelj J, Pišlar A, Šlenc J, Gobec M, Živin M, Tratnjek L, Perše M, Sałat K, Podkowa A, Filipek B, Nachon F, Brazzolotto X, Więckowska A, Malawska B, Stojan J, Raščan IM, Kos J, Coquelle N, Colletier J-P, Gobec S (2016). Development of an in-vivo active reversible butyrylcholinesterase inhibitor. Scientific Reports 6:39495 https://doi.org/10.1038/srep39495

[25]. Kurt BZ, Gazioglu I, Dag A, Salmas RE, Kayık G, Durdagi S, Sonmez F (2017). Synthesis, anticholinesterase activity and molecular modeling study of novel carbamate-substituted thymol/carvacrol derivatives. Bioorganic & Medicinal Chemistry 25:1352-1363 https://doi.org/10.1016/j.bmc.2016.12.037

[26]. Lane RM, Potkin SG, Enz A (2006). Targeting acetylcholinesterase and butyrylcholinesterase in dementia. International Journal of Neuropsychopharmacology 9:101-124 https://doi.org/10.1017/S1461145705005833

[27]. Li H, Robertson AD, Jensen JH (2005). Very fast empirical prediction and rationalization of protein pKa values. Proteins: Structure, Function, and Bioinformatics 61:704-721 https://doi.org/10.1002/prot.20660

[28]. Liston DR, Nielsen JA, Villalobos A, Chapin D, Jones SB, Hubbard ST, Shalaby IA, Ramirez A, Nason D, White WF (2004). Pharmacology of selective acetylcholinesterase inhibitors: implications for use in

Alzheimer's disease. European Journal of Pharmacology 486:9-17 https://doi.org/10.1016/j.ejphar.2003.11.080

[29]. Madhavi Sastry G, Adzhigirey M, Day T, Annabhimoju R, Sherman W (2013). Protein and ligand preparation: parameters, protocols, and influence on virtual screening enrichments. Journal of Computer-Aided Molecular Design 27:221-234 https://doi.org/10.1007/s10822-013-9644-8

[30]. Martyna GJ, Tobias DJ, Klein ML (1994). Constant pressure molecular dynamics algorithms. The Journal of Chemical Physics 101:4177-4189 https://doi.org/10.1063/1.467468

[31]. Matthews KA, Xu W, Gaglioti AH, Holt JB, Croft JB, Mack D, McGuire LC (2019). Racial and ethnic estimates of Alzheimer's disease and related dementias in the United States (2015–2060) in adults aged ≥65 years. Alzheimer's & Dementia 15:17-24 https://doi.org/10.1016/j.jalz.2018.06.3063

[32]. Mirjana BC, Danijela ZK, Tamara DL-P, Aleksandra MB, Vesna MV (2013). Acetylcholinesterase Inhibitors: Pharmacology and Toxicology. Current Neuropharmacology 11:315-335 https://doi.org/10.2174/1570159X11311030006

[33]. Myshkin E, Brennan R, Khasanova T, Sitnik T, Serebriyskaya T, Litvinova E, Guryanov A, Nikolsky Y, Nikolskaya T, Bureeva S (2012). Prediction of Organ Toxicity Endpoints by QSAR Modeling Based on Precise Chemical-Histopathology Annotations. Chemical Biology & Drug Design 80:406-416 https://doi.org/10.1111/j.1747-0285.2012.01411.x

[34]. Nosé S (1984). A unified formulation of the constant temperature molecular dynamics methods. The Journal of Chemical Physics 81:511-519 https://doi.org/10.1063/1.447334

[35]. Ogura H, Kosasa T, Araki S, Yamanishi Y (2000). Pharmacological properties of donepezil hydrochloride (Aricept©), a drug for Alzheimer's disease. Folia Pharmacologica Japonica 115:45-51 https://doi.org/10.1254/fpj.115.45

[36]. Orhan IE, Jedrejek D, Senol FS, Salmas RE, Durdagi S, Kowalska I, Pecio L, Oleszek W (2018). Molecular modeling and in vitro approaches towards cholinesterase inhibitory effect of some natural xanthohumol, naringenin, and acyl phloroglucinol derivatives. Phytomedicine 42:25-33 https://doi.org/10.1016/j.phymed.2018.03.009

[37]. Sahin K, Zengin Kurt B, Sonmez F, Durdagi S (2020). Novel AChE and BChE inhibitors

[38]. using combined virtual screening, text mining and in vitro binding assays. Journal of Biomolecular Structure and Dynamics 38:3342-3358 https://doi.org/10.1080/07391102.2019.1660218

[39]. Shaikh S, Dhavan P, Singh P, Uparkar J, Vaidya SP, Jadhav BL, Ramana MV (2020). Synthesis of carbazole based α-aminophosphonate derivatives: design, molecular docking and in vitro cholinesterase activity. Journal of Biomolecular Structure and Dynamics 1-23 https://doi.org/10.1080/07391102.2020.1861981

[40]. Shelley JC, Cholleti A, Frye LL, Greenwood JR, Timlin MR, Uchimaya M (2007). Epik: a software program for pKaprediction and protonation state generation for drug-like molecules. Journal of Computer-Aided Molecular Design 21:681-691 https://doi.org/10.1007/s10822-007-9133-z

[41]. Sherman W, Day T, Jacobson MP, Friesner RA, Farid R (2006). Novel Procedure for Modeling Ligand/Receptor Induced Fit Effects. Journal of Medicinal Chemistry 49:534-553 https://doi.org/10.1021/jm050540c

[42]. Thompson PA, Wright DE, Counsell CE, Zajicek J (2012). Statistical analysis, trial design and duration in Alzheimer's disease clinical trials: a review. International Psychogeriatrics 24:689-697 https://doi.org/10.1017/S1041610211001116

[43]. Weinstock M (1999). Selectivity of Cholinesterase Inhibition. CNS Drugs 12:307-323 https://doi.org/10.2165/00023210-199912040-00005

[44]. Wu J, Tian Y, Wang S, Pistolozzi M, Jin Y, Zhou T, Roy G, Xu L, Tan W (2017). Design, synthesis and biological evaluation of bambuterol analogues as novel inhibitors of butyrylcholinesterase. European Journal of Medicinal Chemistry 126:61-71 https://doi.org/10.1016/j.ejmech.2016.08.061

[45]. Zilbeyaz K, Stellenboom N, Guney M, Oztekin A, Senturk M (2018). Effects of aryl methanesulfonate derivatives on acetylcholinesterase and butyrylcholinesterase. Journal of Biochemical and Molecular Toxicology 32:e22210 https://doi.org/10.1002/jbt.22210

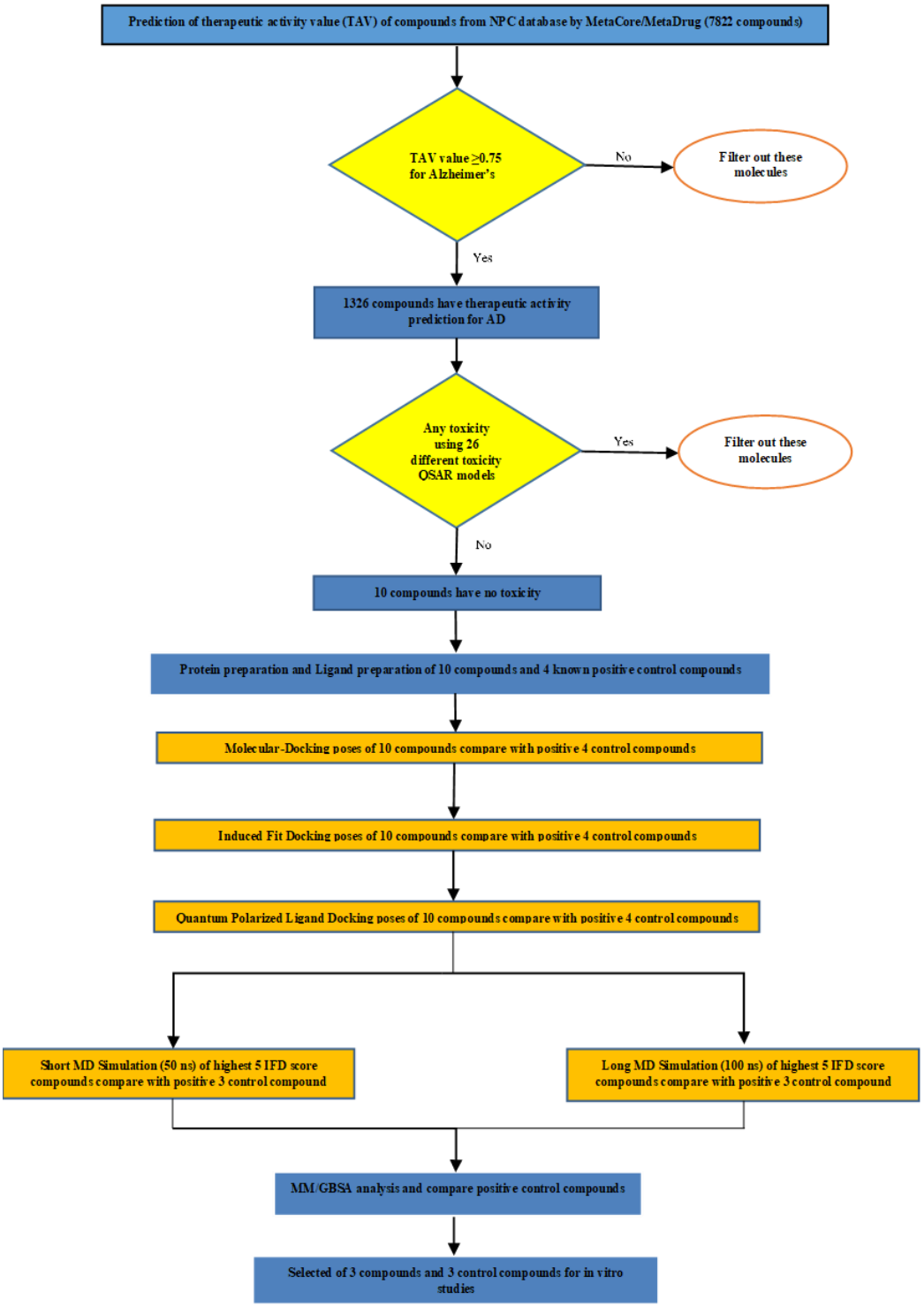

Scheme 1. Conducted virtual screening workflow

Tables

Table 1. Glide/SP, IFD, QPLD and ligand efficiency scores of selected 10 hits and reference compounds with AChE and BChE targets. [a]Model description: Training set: N=261, test set: N=44, Sensitivity: 0.91, Specificity: 0.82, Accuracy: 0.86, Matthews Correlation Coefficient (MCC): 0.73.

Molecules		AChE				BChE			
Selected Hits	Prediction of Therapeutic Activity with AD-QSAR model[a]	Glide/SP (kcal/mol)	Glide/IFD (kcal/mol)	QPLD (kcal/mol)	Ligand Efficiency (kcal/mol)	Glide/SP (kcal/mol)	Glide/IFD (kcal/mol)	QPLD (kcal/mol)	Ligand Efficiency (kcal/mol)
Cafedrine	0.76	-12.37	-17.59	-16.49	-0.68	-8.81	-9.27	-8.44	-0.36
Ocaperidone	0.81	-12.31	-17.76	-15.26	-0.57	-8.72	-10.70	-8.72	-0.35
Isosulpride	0.76	-11.20	-15.02	-15.21	-0.75	-7.60	-11.21	-9.00	-0.49
Risperidone	0.82	-10.23	-17.04	-17.25	-0.57	-8.94	-10.82	-9.11	-0.38
Nelfinavir	0.89	-9.77	-12.60	-11.78	-0.32	-9.80	-13.42	-10.76	-0.34
Podilfen	0.78	-9.10	-11.14	-9.31	-0.46	-7.16	-9.16	-7.47	-0.38
Mafoprazine	0.77	-7.79	-9.38	-9.73	-0.32	-6.70	-8.95	-8.46	-0.31
Tubulozole	0.88	-7.21	-13.37	-8.90	-0.38	-6.48	-9.23	-8.00	-0.28
Montirelin	0.88	-6.05	-10.93	-8.82	-0.39	-7.90	-9.82	-8.46	-0.35
Zolasartan	0.82	-5.12	-11.35	-6.08	-0.32	-7.06	-8.42	-8.52	-0.24
Reference Molecules									
Donepezil		-14.10	-18.65	-19.80	-0.67	-7.88	-11.71	-9.96	-0.42
Neostigmine		-8.84	-12.03	-11.83	-0.75	-6.52	-6.37	-5.62	-0.40
Rivastigmine		-8.54	-10.98	-11.54	-0.61	-5.42	-6.57	-6.42	-0.37

Table 2. AChE and BChE inhibition results (IC_{50}, nM) of selected hit molecules and known inhibitors.

Molecules	AChE (IC_{50}, nM)	BuChE (IC_{50}, nM)
Ocaperidone	89.22 ± 2.67	49.37 ± 1.49
Risperidone	72.30 ± 2.17	46.70 ± 1.39
Nelfinavir	70.23 ± 2.10	36.06 ± 1.08
Neostigmin	135.91 ± 1.12	84.00 ± 0.81
Rivastigmin	60.00 ± 3.11	14.10 ± 0.56
Donepezil	13.40 ± 0.84	844.00 ± 47.9

Figures

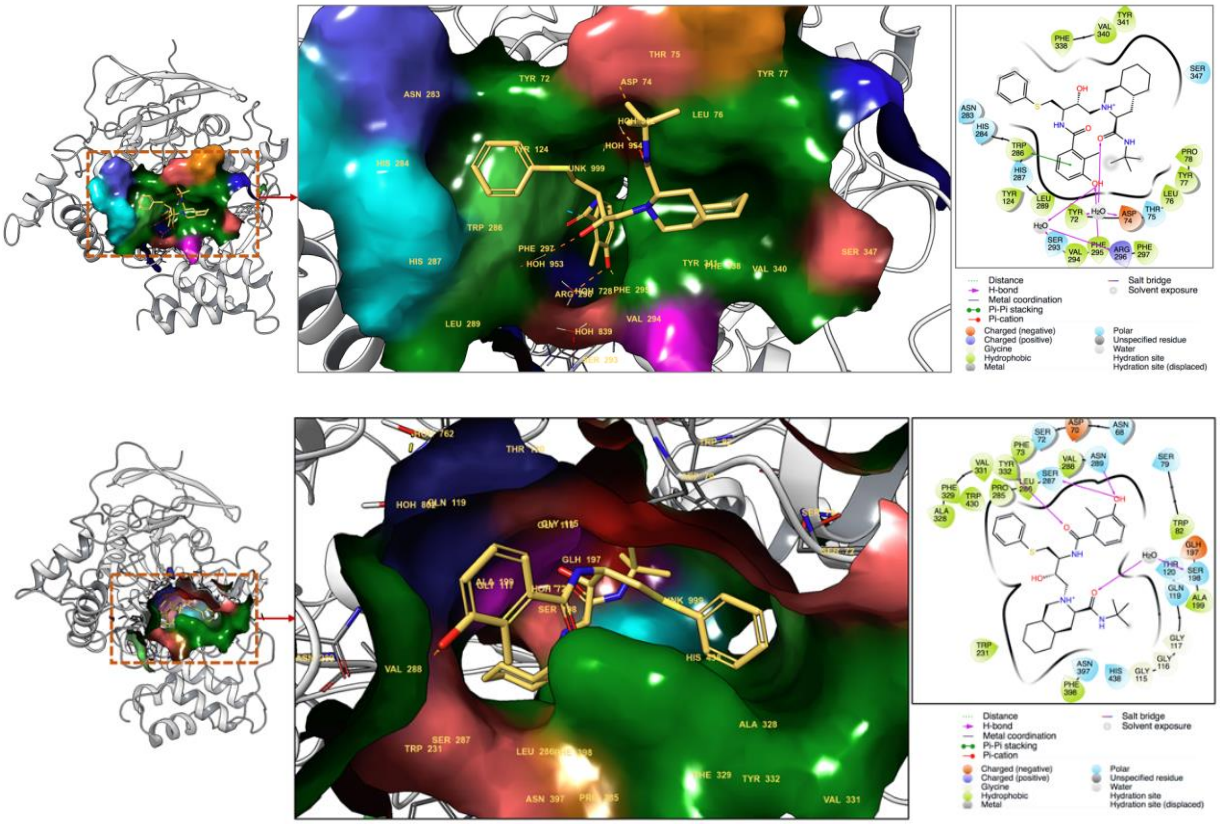

Figure 1. (top) Top-docking pose of nelfinavir at the binding pocket of AChE. (bottom) top-docking pose of nelfinavir at the binding pocket of BChE. 3D (left) and 2D (right) ligand interactions diagrams are represented at the figures.

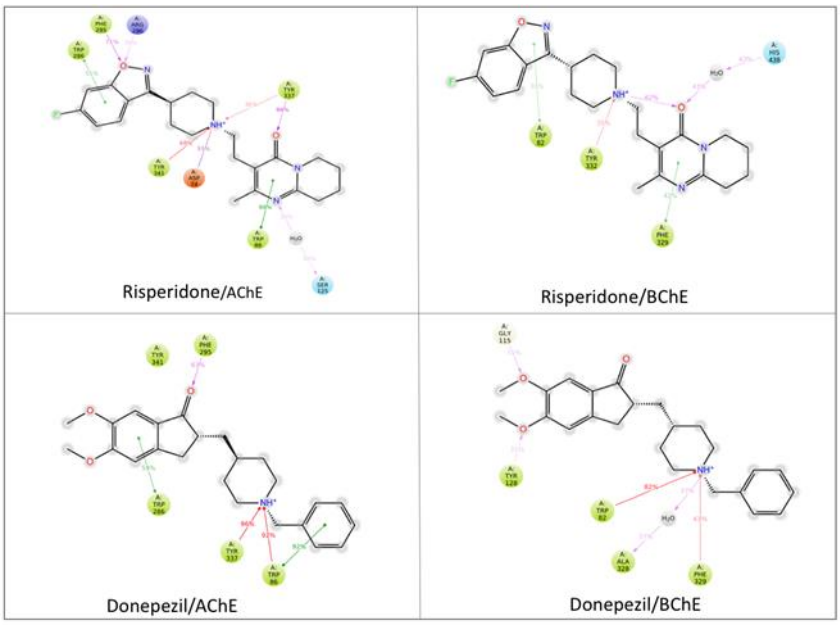

Figure 2. 2D ligand interactions diagrams of risperidone and donepezil at AChE and BChE targets during 100-ns MD simulations.

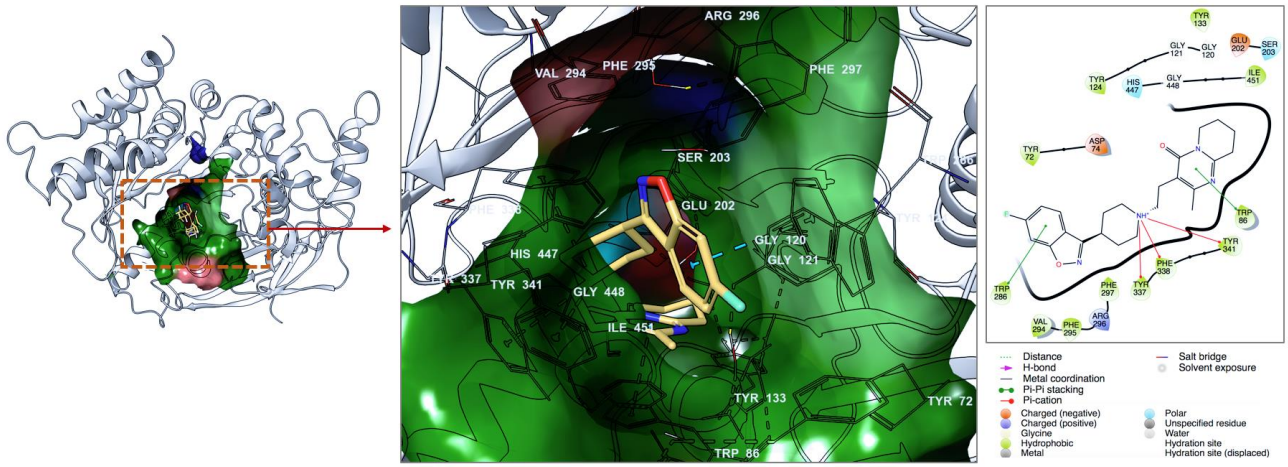

Figure 3. 3D ligand interactions diagram of risperidone at the AChE target. Representative complex structure from 100-ns MD simulations.